5-Aminoimidazole-4-carboxamide riboside (AICAR) enhances GLUT2-dependent jejunal glucose transport: a possible role for AMPK

John WALKER*, Humberto B. JIJON*, Hugo DIAZ*, Payam SALEHI†, Thomas CHURCHILL† and Karen L. MADSEN*[1]

*Division of Gastroenterology, University of Alberta, 6146 Dentistry Pharmacy Building, Edmonton, Alberta, Canada T6G 2C2, and †Department of Surgery, University of Alberta, Edmonton, Alberta, Canada T6G 2C2

AMPK (AMP-activated protein kinase) is a key sensor of energy status within the cell. Activated by an increase in the AMP/ATP ratio, AMPK acts to limit cellular energy depletion by down-regulating selective ATP-dependent processes. The purpose of the present study was to determine the role of AMPK in regulating intestinal glucose transport. [^{3}H]3-*O*-methyl glucose fluxes were measured in murine jejunum in the presence and absence of the AMPK activators AICAR (5-aminoimidazole-4-carboxamide riboside) and metformin and the p38 inhibitor, SB203580. To differentiate between a sodium-coupled (SGLT1) and diffusive (GLUT2) route of entry, fluxes were measured in the presence of the SGLT1 and GLUT2 inhibitors phloridzin and phloretin. Glucose transporter mRNA levels were measured by reverse transcriptase–PCR, and localization by Western blotting. Surface-expressed GLUT2 was assessed by luminal biotinylation. Activation of p38 mitogen-activated protein kinase was analysed by Western blotting. We found that treatment of jejunal tissue with AICAR resulted in enhanced net glucose uptake and was associated with phosphorylation of p38 mitogen-activated protein kinase. Inhibition of p38 abrogated the stimulation of AICAR-stimulated glucose uptake. Phloretin abolished the AICAR-mediated increase in glucose flux, whereas phloridzin had no effect, suggesting the involvement of GLUT2. In addition, AICAR decreased total protein levels of SGLT1, concurrently increasing levels of GLUT2 in the brush-border membrane. The anti-diabetic drug metformin, a known activator of AMPK, also induced the localization of GLUT2 to the luminal surface. We conclude that the activation of AMPK results in an up-regulation of non-energy requiring glucose uptake by GLUT2 and a concurrent down-regulation of sodium-dependent glucose transport.

Key words: 5-aminoimidazole-4-carboxamide riboside (AICAR), AMP-activated protein kinase, glucose, GLUT2, p38, SGLT1.

INTRODUCTION

Maintaining sufficient stores of ATP must be considered as one of the fundamental requirements for cell survival. The myriad of energy-dependent processes requiring ATP includes all types of cellular operations, from gene transcription and translation to osmoregulation. Therefore it is critical for the cell to sense and respond to alterations in energy status. The AMPK (AMP-activated protein kinase) appears to act as a master switch capable of maintaining energy balance within cells by regulating rates of both ATP-consuming and ATP-generating pathways [1]. Present in all eukaryotic cells, AMPK is a serine/threonine kinase that exists as a heterotrimer composed of a catalytic α subunit and regulatory β and γ subunits [2]. Activation of AMPK involves an allosteric mechanism by which AMP binds to AMPK, in addition to phosphorylation of a threonine residue on the catalytic subunit of AMPK catalysed by an upstream kinase, AMPK kinase [3]. Although it was initially thought that AMPK responded only under conditions of metabolic stress as a result of increased intracellular AMP/ATP ratio [4], it is now known that AMPK responds to various stimuli that do not alter ATP levels, suggesting the involvement of other intracellular signalling pathways [5]. Recently, we characterized the role of AMPK in the intestinal epithelium as it pertained to ion secretion through the CFTR (cystic fibrosis transmembrane conductance regulator), and demonstrated that this energy-dependent ion secretory process was inhibited by AMPK [6]. However, the inhibition of energy-consuming processes represents only one-half of the dual mandates of AMPK. The importance of AMPK in activating ATP-producing pathways has been demonstrated in a number of tissues and cell types, including promoting fatty acid oxidation in the liver [7] and in stimulating glucose uptake by skeletal muscles [8,9].

Glucose absorption by the intestinal enterocyte involves at least two modes: transport of glucose coupled with the passage of sodium by the energy-dependent glucose transporter, SGLT1 [10,11], with an apparent K_m of 8–23 mM; and a diffusive route of entry (GLUT2), non-saturable, with a K_m between 30 and 50 mM [12]. Although the appearance of GLUT2 in the BBM (brush-border membrane) had originally been reported in animal models of diabetes, and was presumed to be a pathological adaptation [13], subsequent studies have reported the recruitment of GLUT2 to the BBM as an adaptive measure in response to such stimuli as high luminal glucose concentrations [14], stimulation with PMA [15], and most recently, infusion of the enteric peptide hormone GLP-2 (glucagon-like peptide 2) [16]. Experiments performed in the present study demonstrate that activation of AMPK induces glucose uptake by the intestine by increasing the recruitment of GLUT2 to the BBM, and subsequently decreases total cellular SGLT1 protein levels. We conclude from this study that AMPK promotes glucose uptake by the intestine in an energy-independent fashion while also acting to down-regulate active transport that would further stress an already metabolically compromised cell.

Abbreviations used: ACC, acetyl-CoA carboxylase; AICAR, 5-aminoimidazole-4-carboxamide riboside; AMPK, AMP-activated protein kinase; BBM, brush-border membrane; MAPK, mitogen-activated protein kinase; mTOR, mammalian target of rapamycin; PD, potential difference; RT, reverse transcriptase.

[1] To whom correspondence should be addressed (email karen.madsen@ualberta.ca).

METHODS

Animals

129 Sv/Ev mice were housed behind a barrier under specific pathogen-free conditions. The mice had *ad libitum* access to autoclaved 9 % fat rodent blocs and sterile filtered water. The facility's sanitation was verified by Health Sciences Lab Animal Services at the University of Alberta (Edmonton, Alberta, Canada). All experiments were performed according to the institutional guidelines for the care and use of laboratory animals in research and with the permission of the local ethics committee.

Epithelial glucose uptake

Mice were killed by cervical dislocation, and a 5 cm segment of jejunum 3 cm from the ligament of treitz was removed. Jejunal tissue was mounted in Lucite chambers exposing mucosal and serosal surfaces to 10 ml of oxygenated Krebs buffer (in mmol/l: 115 NaCl, 8 KCl, 1.25 $CaCl_2$, 1.2 $MgCl_2$, 2 KH_2PO_4, 25 $NaHCO_3$, pH 7.35). The buffers were maintained at 37 °C by a heated water jacket and circulated by CO_2/O_2. Fructose (10 mmol/l) was added to the serosal and mucosal sides. The spontaneous transepithelial PD (potential difference) was determined, and the tissue was clamped at zero voltage by continuously introducing an appropriate short-circuit current (I_{sc}) with an automatic voltage clamp (DVC 1000 World Precision Instruments, New Haven, CT, U.S.A.) every 5 min, except for 5–10 s when PD was measured by removing the voltage clamp. Tissue ion conductance (G) was calculated from PD and I_{sc} according to Ohm's law. For the measurement of basal glucose fluxes, the tissue was clamped at zero voltage by continuously introducing an appropriate I_{sc} with an automatic voltage clamp every 5 min, except for 5–10 s when PD was measured by removing the voltage clamp. Tissue pairs were matched for conductance and discarded if conductance varied by > 20 %. The non-metabolizable glucose analogue 3-*O*-methyl-D-[1-^{3}H]glucose (5 μCi; NEN, Boston, MA, U.S.A.) was added either to the serosal or mucosal side after mounting and the tissue was allowed to equilibrate for 20 min. Net directional flux from mucosal-to-serosal surface was determined for conductance-matched tissues by measuring four consecutive 5 min fluxes before the addition of AICAR (5-aminoimidazole-4-carboxamide riboside; 2.5 mM) and four 5 min fluxes following the addition of the AMPK activator. To measure AICAR-dependent glucose transport in conjunction with p38 MAPK (mitogen-activated protein kinase) inhibition, jejunum was incubated with the p38 MAPK inhibitor SB203580 (20 μM) for 30 min before subsequent treatment.

Glucose uptake in response to AICAR is reported as the difference between the averaged values of the four consecutive 5 min fluxes before the addition of the drug and the averaged values of the four consecutive 5 min fluxes post-treatment.

Western blotting

Jejunal mucosa was collected by scraping with a microscope slide and suspended in 0.5 ml Mono-Q buffer. After collection, tissue suspensions were sonicated on ice and protein concentrations were determined by using the Bradford method. Samples were separated by SDS/PAGE and were either Coomassie-stained (to ensure even loading of lanes) or transferred on to PVDF membrane (Millipore). Membranes were blocked for 2 h with 3 % (w/v) skimmed milk-TTBS (20 mM Tris, 0.5 M NaCl, 0.05 % Tween 20, pH 7.4) and incubated overnight at 4 °C with primary antibody (diluted to manufacturer's instructions). Membranes were washed three times with water and incubated for 2 h with goat anti-rabbit secondary antibodies (1:2500 dilution; Bio-Rad), followed by two washes with TTBS. Autoradiography was performed on Kodak X-OMAT AR film using a chemiluminescence kit (Lumi-light; Amersham Biosciences). Five antibodies were employed in this study, recognizing SGLT1 (Chemicon, Temecula, CA, U.S.A.), GLUT2 (Santa Cruz Biotechnologies, Santa Cruz, CA, U.S.A.), AMPK phosphorylated at Thr-172, phospho-ACC (acetyl-CoA carboxylase) and phospho-p38 (all the latter three antibodies were purchased from Cell Signaling Technologies, Beverly, MA, U.S.A.) respectively. Where Western blots are presented as representative data our findings were reproducible in at least two successive experiments.

Biotinylation of surface proteins

Proteins expressed on the apical surface of jejunal enterocytes were labelled with *N*-hydroxysuccinimido (NHS)-SS-biotin (Jackson Immunoresearch Laboratories, West Grove, PA, U.S.A.) and introduced into the intestinal lumen. At the end of the incubation, the intestine was cooled on ice. The luminal solution containing NHS-SS-biotin, 1.5 mg/ml in 10 mM triethanolamine/2.5 mM $CaCl_2$/250 mM sucrose buffer (pH 9.0), was introduced into the lumen and left for 30 min. The lumen was then flushed with a PBS/100 mM glycine buffer to quench the free biotin before two final washings with PBS. Mucosal scrapings were then used to make protein extracts as described below.

Isolation of biotinylated proteins

Proteins were extracted from the homogenate for 1 h at 4 °C using the following buffer: 1.0 % Triton X-100, 150 mM NaCl, 5 mM EDTA and 50 mM Tris (pH 7.5). After centrifugation at 14 000 ***g*** for 10 min, the supernatant was collected and incubated overnight with streptavidin beads. After washing twice with the Triton X-100 buffer to remove non-linked protein, the beads were washed with a high-salt buffer (500 mM NaCl) and finally with a no-salt buffer (10 mM Tris, pH 7.5). The isolated biotinylated proteins were then solubilized in SDS sample buffer to be run on SDS/PAGE for Western blotting. Running samples of the supernatant after spinning down the streptavidin-coated beads on the same Western blots as samples of recovered biotinylated protein made comparisons of total cell GLUT2 with apical GLUT2.

RNA extraction and RT (reverse transcriptase)–PCR

Jejunal mucosa was collected in 1 ml TRIzol® reagent (Gibco BRL). RNA was isolated using a standard phenol/chloroform extraction. Briefly, mucosal scraping was vortex-mixed extensively in TRIzol® before centrifugation at 14 000 ***g*** for 10 min at 4 °C. Chloroform (200 μl) was added to the pellet, the mixture was spun at 12 000 ***g*** for 15 min at 4 °C, and the top layer transferred to a new tube. An equal volume of propan-2-ol was added to extract the RNA, and after centrifugation (12 000 ***g***, 10 min, 4 °C), the pellet was washed once with 75 % ethanol.

cDNA was synthesized using the SuperScript preamplification system (Gibco BRL). Specific oligonucleotide primers were synthesized based on the published sequence for murine SGLT1 [17]. Primer F1 was 5′-GACATCTCAGTCATCGTCATC-3′ (forward) and primer F2 5′-TGTGATTGTATAAAGGGCAGTG-3′ (reverse). PCR conditions were as follows: 94 °C for 2 min; 21 cycles of 94 °C for 1 min, 55 °C for 1 min, 72 °C for 1 min; and 72 °C for 10 min. Amplification of a housekeeping gene, β-actin, was used as an internal PCR control. PCR products were visualized on a 2 % agarose gel with 0.50 μg/ml ethidium bromide.

AMPK activity assay

AMPK enzyme activity was assayed as described previously [6]. Briefly, jejunal segments were excised and epithelial cells isolated using an EDTA/dithiothreitol buffer. Isolated epithelial cells were incubated at 37 °C in a Krebs-Hepes buffer and treated as indicated in the Figure legends. Subsequent to treatment, an equivalent volume of ice-cold homogenization buffer (in mmol/l): 50 Tris/HCl, 250 mannitol, 1 EDTA, 1 EGTA, 50 NaF, 5 $Na_4P_2O_7 \cdot 10\ H_2O$, 1 PMSF, 1 dithiothreitol, and 10 % (v/v) glycerol, 0.1 % Triton X-100 and 1 μl/ml protease inhibitor cocktail (Sigma, St. Louis, MO, U.S.A.) was added directly to the cells before snap-freezing in liquid nitrogen. The crude homogenate was sonicated with 4 pulses of 3 s each before centrifugation at 18 000 ***g*** for 3 min. Protein concentrations were then determined using the Bradford method, and each sample was diluted accordingly to an equivalent protein concentration. To 200 μl of the sample, 2 μl of α-AMPK antibody (Cell Signaling Technologies) was added, and the immunoprecipitation was incubated overnight at 4 °C with gentle mixing. After 12 h immunoprecipitation, 30 μl of Protein A beads (50 % slurry) was added to each sample and incubated for 2 h at 4 °C with gentle mixing. The assay was begun with the addition of immunoprecipitated enzyme to assay buffer {in mM: 80 Hepes buffer, 160 NaCl, 1.6 EDTA, 200 μM SAMS peptide (Alberta Peptide Institute, Edmonton, AB, Canada), 200 μM AMP, 200 μM ATP, 16 % glycerol, 0.1 % Triton X-100 and 0.5 μCi [γ-^{32}P]ATP per sample}. After the addition of enzyme to the reaction tube, samples were vortex-mixed for 5 s and incubated for 10 min at 30 °C. After incubation, the reaction mixture was vortex-mixed and spotted on P81 Whatman filter paper (Fisher Scientific, Pittsburgh, PA, U.S.A.), briefly allowed to dry, and washed three times in 1 % $HClO_4$ before a single wash in acetone. After sufficient time to allow the filter papers to air dry, they were immersed in a scintillant-fluor cocktail and the activity of each sample was measured in a Beckman scintillation counter. Unless otherwise listed, all reagents used in this assay were purchased from Sigma.

Statistical analysis

Results are expressed as means $\pm$ S.E.M., and statistical analyses were performed using the statistical software SigmaStat (Jandel Scientific, San Rafael, CA, U.S.A.). Differences between mean values were evaluated by ANOVA or paired *t* test where appropriate. Specific differences were tested using Student–Newman–Keuls test.

RESULTS

AICAR activates AMPK in jejunal tissue

AICAR has been employed in several studies as an activator of AMPK, but AMPK-independent AICAR responses have also been reported, albeit with less frequency. To assess the activation of AMPK by AICAR in mouse jejunal tissue, mucosal scrapings of tissue incubated with AICAR were examined in Western blots. Both the phosphorylation of AMPK at Thr-172 in response to 2.5 mM AICAR, as well as the phosphorylation of the well-characterized AMPK-substrate ACC was assessed. Phosphorylation of Thr-172 is essential for the AMPK activity, and numerous studies have demonstrated that the activity of AMPK is linked with the phosphorylation status of Thr-172 under all conditions thus far examined [5]. Figure 1(A) demonstrates the time-dependent phosphorylation of both AMPK and ACC in the presence of AICAR. In both experiments, the control group was jejunal tissue treated with vehicle (0.25 % DMSO) for the maximum incubation period represented in the AICAR group. Phosphorylation of both AMPK and ACC was evident by 15 min, and increased in intensity after 30 and 45 min, suggesting that AICAR activates AMPK in murine jejunal tissue.

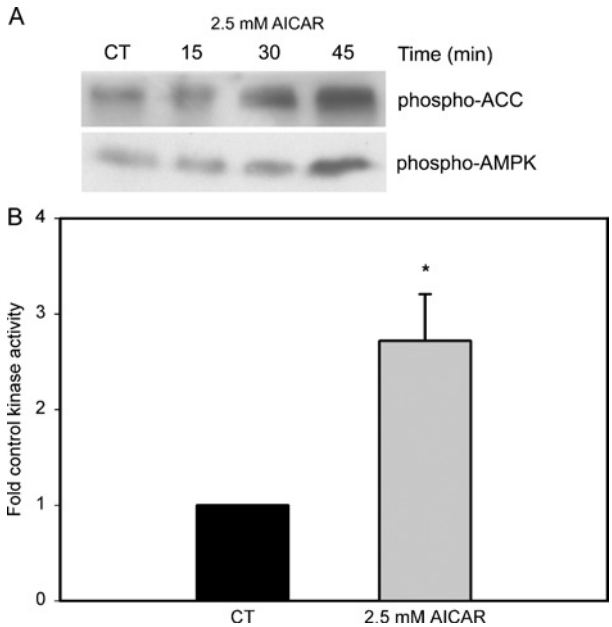

Figure 1 Time-dependent phosphorylation and activation of AMPK and phosphorylation of ACC with treatment by AICAR

(**A**) Western blot of isolated jejunum incubated with 2.5 mM AICAR at 37 °C in oxygenated normal Ringer's solution for the time period indicated. In both experiments, the control group was jejunal tissue treated with vehicle (0.25 % DMSO) for the maximum incubation period represented in the AICAR group. After treatment, mucosal scrapings were analysed by Western blot for the phosphorylation state of the indicated targets. (**B**) AMPK activity assay of isolated jejunum incubated with 2.5 mM AICAR (30 min treatment). The control group was jejunal tissue treated with vehicle (0.25 % DMSO). Error bars represent S.E.M. Significance was determined by unpaired Student's *t* test (*$P < 0.05$, $n = 5$). CT, control.

In Figure 1(B), the effect of AICAR treatment on AMPK activity is directly demonstrated by means of a kinase assay. As measured in isolated murine jejunal epithelial cells, with 30 min incubation (2.5 mM) the activity of the kinase is increased by more than 2-fold (2.7 ± 0.49) compared with vehicle-treated cells.

Effect of AICAR on jejunal glucose transport

Serosally added AICAR (2.5 mM) resulted in a 2.2-fold increase in net stimulated jejunal 3-*O*-methyl glucose uptake (Figure 2A). The use of the glucose transport inhibitors phloridzin and phloretin were used to discriminate between the relative contributions of the SGLT1 and GLUT2 transporters to basal and stimulated jejunal glucose absorption. In the absence of AICAR under basal conditions, both inhibitors reduced basal uptake by $\geqslant 50$ % suggesting that under our *in vitro* conditions, both SGLT1 and GLUT2 contributed to jejunal glucose transport. In Figure 2(B) it can be seen that the presence of the SGLT1 inhibitor, phloridzin, had no effect on the ability of AICAR to stimulate net glucose flux. Glucose flux increased by approx. 1.7-fold compared with that obtained for phloridzin alone. In contrast, the presence of the GLUT2 inhibitor, phloretin, entirely abrogated the ability of AICAR to increase net glucose flux (Figure 2C), suggesting that the up-regulation of glucose transport induced by AICAR involved GLUT2-mediated transport mechanisms. Interestingly, the presence of both AICAR and phloretin resulted in almost a complete ablation of jejunal glucose transport (Figure 2C),

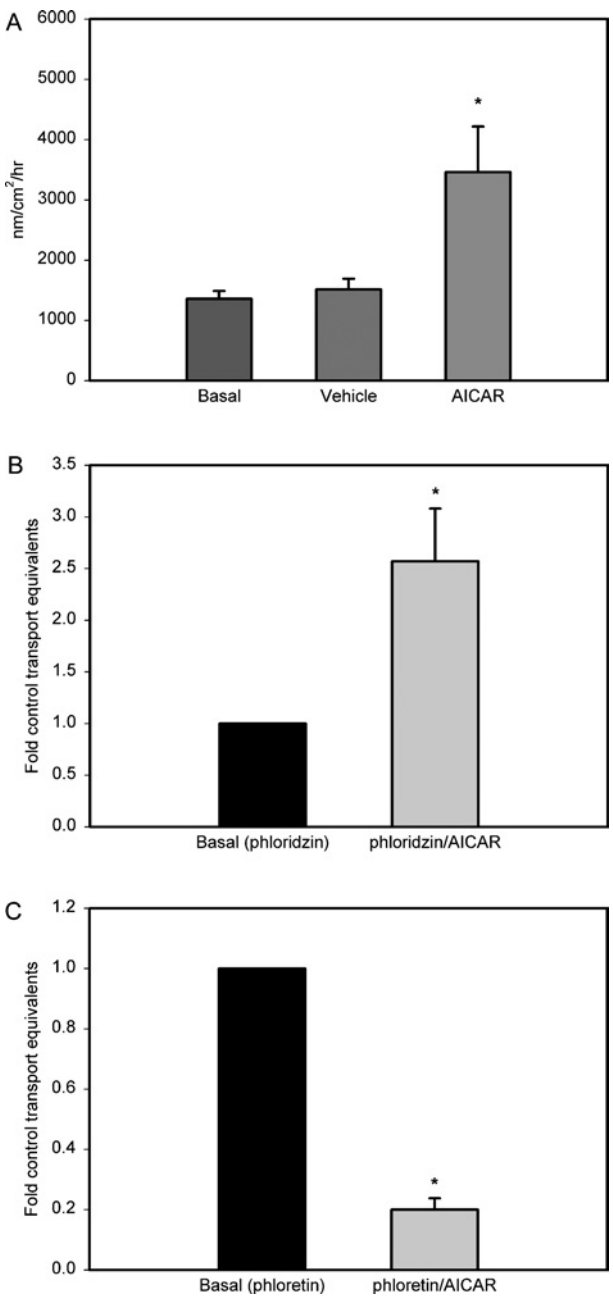

Figure 2 Uptake of 3-*O*-methyl glucose from isolated jejunal tissue

(**A**) Jejunal tissue was mounted in Lucite chambers exposing mucosal and serosal surfaces to 10 ml of oxygenated Krebs buffer. Net directional 3-*O*-methyl glucose flux from mucosal-to-serosal surface was determined by measuring four consecutive 5 min fluxes before the addition of AICAR (2.5 mM) and four 5 min fluxes after the addition of the AMPK activator. (**B**) Values represent net directional flux as measured in (**A**), except in the presence of the SGLT1 inhibitor phloridzin (1 mM). (**C**) Values represent net directional flux as measured in (**A**), except in the presence of the GLUT2 inhibitor phloretin (1 mM). Error bars represent S.E.M. Significance was determined by ANOVA (**A**) or unpaired Student's *t* test (**B**, **C**), and groups found to be statistically distinct from control are denoted by asterisk ($*P < 0.05$, $n \geqslant 5$ animals per group).

presumably occurring as a result of phloretin-mediated inhibition of luminally localized GLUT2 concurrent with the down-regulation of SGLT1 by AICAR.

SGLT1 protein and mRNA levels in response to AICAR

To confirm that the AICAR-induced increase in net glucose flux did not involve SGLT1-dependent transport, we examined cellular

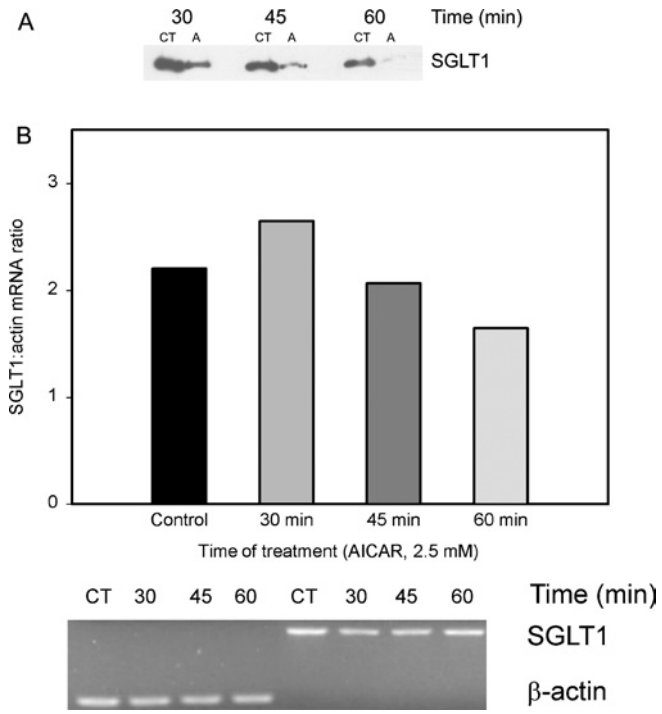

Figure 3 Alterations in SGLT1 transporter and mRNA levels in response to AICAR incubation

(**A**) Western blot of isolated jejunum incubated with 2.5 mM AICAR at 37 °C in oxygenated normal Ringer's solution for the time period indicated. The control group was jejunal tissue treated with vehicle (0.25 % DMSO) for the respective incubation period represented in the AICAR group. After treatment, mucosal scrapings were analysed by Western blot for total cellular levels of SGLT1. (**B**) RT–PCR experiment examining the level of SGLT1 mRNA following incubation of isolated jejunal tissue with 2.5 mM AICAR at 37 °C in oxygenated normal Ringer's solution for the time periods indicated. Values are expressed as the ratio of amplified SGLT1/β-actin cDNA. Differences indicated between treatment groups were not found to be statistically different. CT, control; A, AICAR.

mRNA levels and total protein levels of SGLT1. As seen in Figure 3(A), AICAR treatment of jejunal tissue results in a significant decrease in transporter protein levels. At the earliest time-point examined (30 min), total cellular SGLT1 is significantly reduced, and reduction continues as incubation time with AICAR increases. In 60 min, the transporter is nearly undetectable in comparison with vehicle-incubated tissue. To determine if the alterations in SGLT1 protein levels involved an effect at the transcriptional level, mRNA for SGLT1 was assessed by RT–PCR. As seen in Figure 3(B), there was no significant effect of AICAR on SGLT1 mRNA. This lack of effect of AICAR on SGLT1 mRNA suggests that an alternative regulatory mechanism may have been stimulated by AICAR that involved either alterations in SGLT1 mRNA translation or protein degradation.

Effect of AICAR on GLUT2 localization

Together, the findings that phloridzin did not inhibit AICAR-stimulated glucose jejunal uptake combined with the observation that AICAR decreases SGLT1 transporter levels suggested the involvement of GLUT2 in AICAR-stimulated glucose uptake. Previous studies have reported that glucose absorption in the intestine can be enhanced by the translocation of GLUT2 to the apical membrane [12,15,16]. To assess the possibility that this might be a contributing mechanism to AICAR-dependent absorption, luminal proteins were labelled with biotin, extracted and examined by Western blotting. As can be seen in Figure 4,

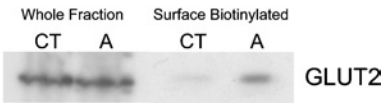

Figure 4 Alterations in total cellular and brush-border-localized GLUT2 in response to AICAR incubation

Western blot of isolated jejunum incubated with 2.5 mM AICAR at 37 °C in oxygenated normal Ringer's solution for 45 min. Luminal proteins were labelled with biotin and examined by Western blotting for alterations in GLUT2 protein. Those lanes labelled 'Whole Fraction' are representative of the tissue preparation before the extraction of the biotinylated proteins, and are taken as indicative of total cellular levels of GLUT2. Lanes labelled 'Surface Biotinylated' are representative of isolated biotinylated proteins, and are representative of surface-expressed GLUT2. The control group was jejunal tissue treated with vehicle (0.25 % DMSO) for an incubation period equivalent to the treatment groups. CT, control; A, AICAR.

incubation with AICAR induces no discernable alteration in the amount of total cellular GLUT2. However, when surface-localized proteins were examined for the presence of GLUT2, we observed a significant increase in the amount of GLUT2 found in the brush-border fraction in the presence of AICAR. This would suggest that the increase in net glucose flux occurred as a function of increased insertion of GLUT2 into the BBM.

p38 MAPK activation is required for AICAR-stimulated glucose transport

Previous studies have suggested that p38 MAPK activation results in increased GLUT2 levels in the BBM [15]. To determine if p38 MAPK was involved in the up-regulation of glucose flux induced by AICAR in jejunal tissue, we examined phosphorylation of the kinase in response to treatment with AICAR. As seen in Figure 5(A), at 30 min, AICAR treatment resulted in enhanced phosphorylation, suggesting that p38 MAPK was activated by AICAR. To investigate the role of p38 MAPK, jejunal tissue was pretreated with 20 μM SB203580, a p38 MAPK inhibitor, and subsequently treated with AICAR. As seen in Figure 5(B), treatment with 20 μM SB203580 significantly attenuated the stimulation of glucose transport in response to AICAR, strongly suggesting a role for p38 MAPK in modulating GLUT2 response to AICAR. SB203580 alone did not alter jejunal glucose transport to a statistically significant degree, although a slight reduction was observed. This is in keeping with the demonstrated role of p38 MAPK in stimulating intrinsic basal transporter activity, as seen in GLUT4 regulation [35].

Effect of the p38 MAP kinase inhibitor, SB203580, on AMPK activation and translocation of GLUT2

Since previous studies [40] have shown SB203580 to inhibit nucleoside transport, we assessed AMPK activation (by ACC phosphorylation) under the same conditions that were used for glucose transport (30 min SB203580 pretreatment followed by AICAR stimulation) to ensure that the ability of SB203580 to inhibit the AICAR-induced effect was not due to a reduction in AICAR entry. As illustrated by Western-blot analysis in Figure 5(C), SB203580 did not alter phosphorylation of the AMPK substrate ACC in response to AICAR, suggesting that AICAR was still capable of activating AMPK in the presence of SB203580.

To identify the role of p38 MAPK in modulating AMPK-dependent glucose uptake, we examined GLUT2 translocation to the BBM in the presence of the p38 inhibitor SB203580. As seen in Figure 6, inhibition of p38 MAPK did not prevent AICAR-dependent GLUT2 translocation, suggesting that the role of p38 MAPK in modulating glucose transport may be a post-translocation event.

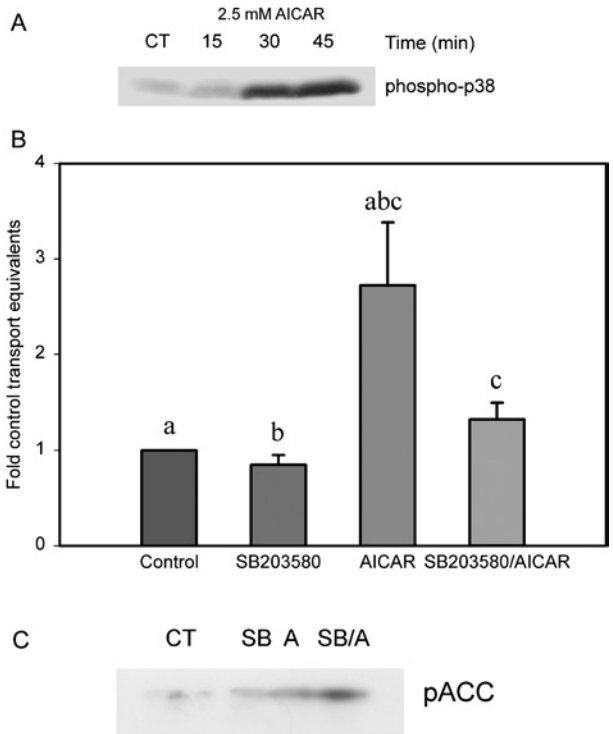

Figure 5 p38 MAPK phosphorylation is required for AICAR-stimulated glucose transport

(**A**) Western blot of isolated jejunum incubated with 2.5 mM AICAR at 37 °C in oxygenated normal Ringer's solution for the time periods indicated. The control group was jejunal tissue treated with vehicle (0.25 % DMSO) for the maximum incubation period represented in the AICAR group. Mucosal scrapings were analysed for phospho-p38 MAPK. (**B**) Net directional 3-*O*-methyl glucose flux from mucosal-to-serosal before, and after the addition of AICAR (2.5 mM). Where treatment involved the p38 inhibitor SB203580 (20 μM) the jejunum was perfused *in vivo* for a period of 30 min before the analysis of *in vitro* glucose transport as described in all other transport experiments. Error bars represent S.E.M. Significance was determined by ANOVA; groups found to be statistically distinct from one another share the same letter (a and b, $P < 0.01$; c, $P < 0.05$, $n \geqslant 5$ animals per group). (**C**) Western blot of isolated jejunum incubated with 2.5 μM AICAR and/or SB203580 (20 μM) showing phosphorylation of the AMPK substrate ACC (phospho-ACC). The control group was jejunal tissue treated with vehicle (0.25 % DMSO) for a period equivalent to the treatment groups. CT, control; A, AICAR; SB, SB203580.

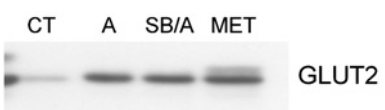

Figure 6 AICAR-dependent GLUT2 translocation to the apical surface is not dependent on p38 MAPK

Western blot of isolated jejunal tissue incubated with 2.5 mM AICAR (30 min) at 37 °C in oxygenated normal Ringer's solution with and without 30 min pretreatment with the p38 inhibitor SB203580 (20 μM). Treatment by the AMPK activator metformin (5 mM) was performed as with AICAR. The control group was jejunal tissue treated with vehicle (0.25 % DMSO) for an incubation period equivalent to the treatment groups. Lanes are representative of isolated biotinylated proteins and are representative of surface-expressed GLUT2. CT, control; A, AICAR; SB, SB203580; MET, metformin.

To reinforce our hypothesis that GLUT2 translocation to the BBM is attributable to AMPK activation, Figure 6 also includes jejunal tissue treated with the anti-diabetic drug metformin, a known activator of AMPK. The mechanism of activation of AMPK by metformin was recently described in [18] and is independent of the mechanism by which AICAR activates AMPK. Our results indicate that metformin is a potent inducer of GLUT2

translocation to the BBM, data that is in keeping with a 1994 report indicating a role for GLUT2 in luminal glucose clearance in response to treatment with metformin [19].

DISCUSSION

In the present study, we have demonstrated that the activation of AMPK with AICAR in murine jejunal tissue results in an increase in net glucose flux that can be attributed to an increased amount of GLUT2 in the BBM. Glucose is actively absorbed across the intestinal epithelium by a sodium-dependent mechanism. The rate-limiting step in absorption is sodium-coupled uptake of the solute at the apical membrane, which is driven by the electrochemical gradient for sodium maintained by the basolateral Na/K-ATPase pump [20]. Sodium must be extruded from the cell by Na/K-ATPase to maintain the sodium gradient; by virtue of this, all sodium-coupled solute absorption requires an input of cellular energy. Hence, under conditions of metabolic stress the cell faces a conundrum; it is imperative that cellular nutrient uptake, and therefore ATP levels, are increased, but the absorptive process is an energy-dependent process. However, in responding to an ATP deficit, by altering the localization of a diffusive, high-capacity glucose transporter, the cell circumvents this dilemma such that GLUT2 facilitates glucose absorption by an energy-independent mechanism.

Results presented in this study strongly support our hypothesis that the activation of AMPK results in enhanced glucose flux by a non-energy-dependent mechanism involving GLUT2. This is evidenced by the observation that AICAR-stimulated glucose uptake was inhibited by phloretin, but not phloridzin, suggesting that SGLT1 was not involved. Furthermore, the finding that levels of biotinylated GLUT2 were increased in the BBM in response to two AMPK activators also supports the hypothesis that GLUT2 responds to AMPK activation. Previous immunohistochemistry studies have shown that a substantial amount of GLUT2 protein can be seen lying just below the brush-border surface in the region of the terminal web, and is rapidly inserted into the apical membrane in response to either high luminal glucose loads or the presence of GLP-2 [16,21]. We extend these findings to demonstrate that GLUT2 insertion into the BBM also occurs in response to AMPK activation. Interestingly, a 1994 study examining the effect of the anti-diabetic drug metformin on intestinal glucose transport demonstrated increased glucose disappearance from the jejunal lumen, as evidenced by the enhanced uptake of 2-deoxy-D-glucose. The choice of a GLUT2-selective substrate suggested the involvement of GLUT2 rather than SGLT1 [19]. Not until 2001, however, was it demonstrated that AMPK activation was a primary mechanism of metformin action [22]. That AMPK acts in this fashion suggests an elegant, effective response to a potential multitude of intestinal pathologies where energy metabolite levels are altered.

In addition to AICAR effects on GLUT2 localization, incubating tissue with AICAR significantly decreased levels of cellular SGLT1, but had no effect on mRNA levels, indicating that under the conditions of our study transcriptional inhibition of SGLT1 did not occur. AMPK has been well documented as a regulator of transcriptional activity [23,24]. In their recent studies, Wang et al. [25,26] proposed a novel function for AMPK as a regulator of cytoplasmic HuR protein levels, which in turn influenced the mRNA-stabilizing function of HuR and the stability of HuR target transcripts. Importantly, HuR has been demonstrated to bind a stabilizing domain in the 3′-untranslated region of SGLT1 mRNA [27]. In the light of this, both destabilization of SGLT1 mRNA and inhibition of translation may be contributing factors to SGLT1 protein down-regulation. However, given the relative abundance of SGLT1 mRNA remaining after 60 min of AICAR incubation, post-transcriptional events are more probable to play a significant role in the reduction in total cellular SGLT1. Recent reports in the literature indicate a possible linkage between AMPK and the mTOR (mammalian target of rapamycin) signalling pathway [28,29]. mTOR is a serine/threonine kinase that functions as a central element involved in the control of cell growth and development [30]. AICAR-mediated inhibition of mTOR-dependent translation is a possible mechanism that would explain the discrepancy between mRNA and total cellular protein levels. Further studies are required to resolve this.

Whereas the activation of p38 MAPK has been linked with AMPK-mediated alterations in glucose transport, the exact nature of the cross-talk between these two pathways, and the role played by p38 MAPK in modulating AMPK-dependent glucose transport is less clear [31,32]. AMPK activation and p38 MAPK activity have been associated in a number of systems [33]. Furthermore, the inhibition of p38 MAPK with SB203580 has previously been shown to inhibit the effect of AICAR on glucose uptake in Clone 9 cells [34]. Our results are similar to those of Xi et al. [34], in that inhibiting p38 MAPK attenuated the AICAR-stimulation of glucose flux in our system. Interestingly, studies by Helliwell et al. [15] demonstrated that activating p38 MAPK in intestinal tissue resulted in enhanced GLUT2 levels and activity in the BBM. They postulated that the observed increase in intestinal hexose absorption induced by physiological stress could be mediated by p38 MAPK. Our findings include a prominent role for p38 in regulating AMPK-dependent glucose transport, but it would seem that this role would exclude participation in the translocation of GLUT2 to the BBM. We demonstrated that AICAR induces GLUT2 translocation to the BBM even in the face of p38 inhibition, suggesting instead that the role of p38, as it pertains to AMPK, in regulating glucose transport is intrinsic to transporter activity. In a related study, Somwar et al. [35] report that activation of GLUT4 (an SB203580-sensitive event) follows GLUT4 translocation to the BBM and that both mechanisms contribute to the stimulation of glucose uptake by insulin in muscles. Our findings suggest that a mechanism similar to the one proposed by Somwar et al. [35] could be extended to the regulation of GLUT2 in the intestine.

Evidence that p38 MAPK effects on intestinal glucose transport did not involve regulation of the AMPK-dependent translocation event suggests that p38 MAPK activation occurred either downstream of or parallel to AMPK activation. Interestingly, our findings also imply a more complex relationship of cross-talk between the respective kinase pathways, as inhibition of p38 MAPK, in and of itself, appeared to be sufficient to activate AMPK. Furthermore, simultaneous p38 MAPK inhibition and AICAR stimulation appeared to potentiate phosphorylation of the AMPK substrate ACC.

AMPK appears to have a role in regulating whole body energy metabolism as well as serum glucose levels, in such a way that activation of AMPK results in enhanced glucose uptake by skeletal muscles [7], increased fatty acid oxidation in skeletal muscles and liver [8,9] and inhibition of glucose production by the liver [36]. Furthermore, AMPK is involved in the regulation of insulin secretion and insulin gene expression [37], and also appears to have a critical role in regulating food intake [38]. Our results demonstrate that AMPK activation in the intestine also enhances net glucose uptake; thus, it is possible that AMPK activity in the intestine may have a critical role in contributing to the control of whole body energy metabolism. Although the use of 3-*O*-methyl glucose in our study does not allow for the examination of intestinal glucose utilization, as this is a non-metabolizable sugar, previous studies examining the effect of metformin, another

activator of AMPK, have shown that metformin increases glucose utilization by the intestine, which would contribute to a decrease in serum glucose levels [39].

In conclusion, it is becoming clear that AMPK-mediated adaptive and physiological responses occur in all tissues, with the end result being maintenance of overall body energy balance. The intestine is probably an important component to this balance, with AMPK activity playing a critical role in regulating nutrient and ion transport under both normal and pathological conditions.

K. L. M. is supported by the Alberta Heritage Foundation for Medical Research as a senior scholar. H. B. J. is supported by AstraZeneca Canada, Canadian Institutes for Health Research (CIHR) and Canadian Association of Gastroenterology as a postdoctoral fellow. Operating grant supports were provided by Canadian Institutes for Health Research, Crohn's and Colitis Foundation of Canada and Alberta Foundation for Medical Research.

REFERENCES

1 Hardie, D. G., Scott, J. W., Pan, D. A. and Hudson, E. R. (2003) Management of cellular energy by the AMP-activated protein kinase system. FEBS Lett. **546**, 113–120
2 Carling, D., Clarke, P. R., Zammit, V. A. and Hardie, D. G. (1989) Purification and characterization of the AMP-activated protein kinase. Copurification of acetyl-CoA carboxylase kinase and 3-hydroxy-3-methylglutaryl-CoA reductase kinase activities. Eur. J. Biochem. **186**, 129–136
3 Stein, S. C., Woods, A., Jones, N. A., Davison, M. D. and Carling, D. (2000) The regulation of AMP-activated protein kinase by phosphorylation. Biochem. J. **345**, 437–443
4 Kemp, B. E., Stapleton, D., Campbell, D. J., Chen, Z. P., Murthy, S., Walter, M., Gupta, A., Adams, J. J., Katsis, F., van Denderen, B. et al. (2003) AMP-activated protein kinase, super metabolic regulator. Biochem. Soc. Trans. **31**, 162–168
5 Carling, D. (2004) AMPK. Curr. Biol. **14**, R220
6 Walker, J., Jijon, H. B., Churchill, T., Kulka, M. and Madsen, K. L. (2003) Activation of AMP-activated protein kinase reduces cAMP-mediated epithelial chloride secretion. Am. J. Physiol. Gastrointest. Liver Physiol. **285**, G850–G860
7 Velasco, G., Geelen, M. J. and Guzman, M. (1997) Control of hepatic fatty acid oxidation by 5′-AMP-activated protein kinase involves a malonyl-CoA-dependent and a malonyl-CoA-independent mechanism. Arch. Biochem. Biophys. **337**, 169–175
8 Merrill, G. F., Kurth, E. J., Hardie, D. G. and Winder, W. W. (1997) AICA riboside increases AMP-activated protein kinase, fatty acid oxidation, and glucose uptake in rat muscle. Am. J. Physiol. **273**, E1107–E1112
9 Fryer, L. G., Foufelle, F., Barnes, K., Baldwin, S. A., Woods, A. and Carling, D. (2002) Characterization of the role of the AMP-activated protein kinase in the stimulation of glucose transport in skeletal muscle cells. Biochem. J. **363**, 167–174
10 Ikeda, T. S., Hwang, E. S., Coady, M. J., Hirayama, B. A., Hediger, M. A. and Wright, E. M. (1989) Characterization of a Na+/glucose cotransporter cloned from rabbit small intestine. J. Membr. Biol. **110**, 87–95
11 Hediger, M. A., Coady, M. J., Ikeda, T. S. and Wright, E. M. (1987) Expression cloning and cDNA sequencing of the Na+/glucose co-transporter. Nature (London) **330**, 379–381
12 Kellett, G. L. and Helliwell, P. A. (2000) The diffusive component of intestinal glucose absorption is mediated by the glucose-induced recruitment of GLUT2 to the brush-border membrane. Biochem. J. **350**, 155–162
13 Corpe, C. P., Basaleh, M. M., Affleck, J., Gould, G., Jess, T. J. and Kellett, G. L. (1996) The regulation of GLUT5 and GLUT2 activity in the adaptation of intestinal brush-border fructose transport in diabetes. Pflugers Arch. **432**, 192–201
14 Gouyon, F., Caillaud, L., Carriere, V., Klein, C., Dalet, V., Citadelle, D., Kellett, G. L., Thorens, B., Leturque, A. and Brot-Laroche, E. (2003) Simple-sugar meals target GLUT2 at enterocyte apical membranes to improve sugar absorption: a study in GLUT2-null mice. J. Physiol. (Cambridge, U.K.) **552**, 823–832
15 Helliwell, P. A., Richardson, M., Affleck, J. and Kellett, G. L. (2000) Stimulation of fructose transport across the intestinal brush-border membrane by PMA is mediated by GLUT2 and dynamically regulated by protein kinase C. Biochem. J. **350**, 149–154
16 Au, A., Gupta, A., Schembri, P. and Cheeseman, C. I. (2002) Rapid insertion of GLUT2 into the rat jejunal brush-border membrane promoted by glucagon-like peptide 2. Biochem. J. **367**, 247–254
17 Tabatabai, N. M., Blumenthal, S. S., Lewand, D. L. and Petering, D. H. (2003) Mouse kidney expresses mRNA of four highly related sodium-glucose cotransporters: regulation by cadmium. Kidney Int. **64**, 1320–1330
18 Zou, M. H., Kirkpatrick, S. S., Davis, B. J., Nelson, J. S., Wiles, I. W., Schlettner, U., Neumann, D., Brownlee, M., Freeman, M. B. and Goldman, M. H. (2004) Activation of the AMP-activated protein kinase by the anti-diabetic drug metformin *in vivo*: role of mitochondrial reactive nitrogen species. J. Biol. Chem. **279**, 43940–43951
19 Bailey, C. J., Mynett, K. J. and Page, T. (1994) Importance of the intestine as a site of metformin-stimulated glucose utilization. Br. J. Pharmacol. **112**, 671–675
20 Thomson, A. B. and Wild, G. (1997) Adaptation of intestinal nutrient transport in health and disease. Part I. Dig. Dis. Sci. **42**, 453–469
21 Affleck, J. A., Helliwell, P. A. and Kellett, G. L. (2003) Immunocytochemical detection of GLUT2 at the rat intestinal brush-border membrane. J. Histochem. Cytochem. **51**, 1567–1574
22 Zhou, G., Myers, R., Li, Y., Chen, Y., Shen, X., Fenyk-Melody, J., Wu, M., Ventre, J., Doebber, T., Fujii, N. et al. (2001) Role of AMP-activated protein kinase in mechanism of metformin action. J. Clin. Invest. **108**, 1167–1174
23 Lee, M., Hwang, J. T., Lee, H. J., Jung, S. N., Kang, I., Chi, S. G., Kim, S. S. and Ha, J. (2003) AMP-activated protein kinase activity is critical for hypoxia-inducible factor-1 transcriptional activity and its target gene expression under hypoxic conditions in DU145 cells. J. Biol. Chem. **278**, 39653–39661
24 Leff, T. (2003) AMP-activated protein kinase regulates gene expression by direct phosphorylation of nuclear proteins. Biochem. Soc. Trans. **31**, 224–227
25 Wang, W., Fan, J., Yang, X., Furer-Galban, S., Lopez de Silanes, I., von Kobbe, C., Guo, J., Georas, S. N., Foufelle, F., Hardie, D. G. et al. (2002) AMP-activated kinase regulates cytoplasmic HuR. Mol. Cell. Biol. **22**, 3425–3436
26 Wang, W., Yang, X., Lopez de Silanes, I., Carling, D. and Gorospe, M. (2003) Increased AMP:ATP ratio and AMP-activated protein kinase activity during cellular senescence linked to reduced HuR function. J. Biol. Chem. **278**, 27016–27023
27 Loflin, P. and Lever, J. E. (2001) HuR binds a cyclic nucleotide-dependent, stabilizing domain in the 3′ untranslated region of Na(+)/glucose cotransporter (SGLT1) mRNA. FEBS Lett. **509**, 267–271
28 Kimura, N., Tokunaga, C., Dalal, S., Richardson, C., Yoshino, K., Hara, K., Kemp, B. E., Witters, L. A., Mimura, O. and Yonezawa, K. (2003) A possible linkage between AMP-activated protein kinase (AMPK) and mammalian target of rapamycin (mTOR) signalling pathway. Genes Cells **8**, 65–79
29 Inoki, K., Zhu, T. and Guan, K. L. (2003) TSC2 mediates cellular energy response to control cell growth and survival. Cell (Cambridge, Mass.) **115**, 577–590
30 Gingras, A. C., Raught, B. and Sonenberg, N. (2004) mTOR signaling to translation. Curr. Top. Microbiol. Immunol. **279**, 169–197
31 Bazuine, M., Ouwens, D. M., Gomes de Mesquita, D. S. and Maassen, J. A. (2003) Arsenite stimulated glucose transport in 3T3-L1 adipocytes involves both Glut4 translocation and p38 MAPK activity. Eur. J. Biochem. **270**, 3891–3903
32 Sweeney, G., Somwar, R., Ramlal, T., Volchuk, A., Ueyama, A. and Klip, A. (1999) An inhibitor of p38 mitogen-activated protein kinase prevents insulin-stimulated glucose transport but not glucose transporter translocation in 3T3-L1 adipocytes and L6 myotubes. J. Biol. Chem. **274**, 10071–10078
33 Lemieux, K., Konrad, D., Klip, A. and Marette, A. (2003) The AMP-activated protein kinase activator AICAR does not induce GLUT4 translocation to transverse tubules but stimulates glucose uptake and p38 mitogen-activated protein kinases alpha and beta in skeletal muscle. FASEB J. **17**, 1658–1665
34 Xi, X., Han, J. and Zhang, J. Z. (2001) Stimulation of glucose transport by AMP-activated protein kinase via activation of p38 mitogen-activated protein kinase. J. Biol. Chem. **276**, 41029–41034
35 Somwar, R., Kim, D. Y., Sweeney, G., Huang, C., Niu, W., Lador, C., Ramlal, T. and Klip, A. (2001) GLUT4 translocation precedes the stimulation of glucose uptake by insulin in muscle cells: potential activation of GLUT4 via p38 mitogen-activated protein kinase. Biochem. J. **359**, 639–649
36 Winder, W. W. and Hardie, D. G. (1999) AMP-activated protein kinase, a metabolic master switch: possible roles in type 2 diabetes. Am. J. Physiol. **277**, E1–E10
37 Salt, I. P., Johnson, G., Ashcroft, S. J. and Hardie, D. G. (1998) AMP-activated protein kinase is activated by low glucose in cell lines derived from pancreatic beta cells, and may regulate insulin release. Biochem. J. **335**, 533–539
38 Minokoshi, Y., Alquier, T., Furukawa, N., Kim, Y. B., Lee, A., Xue, B., Mu, J., Foufelle, F., Ferre, P., Birnbaum, M. J. et al. (2004) AMP-kinase regulates food intake by responding to hormonal and nutrient signals in the hypothalamus. Nature (London) **428**, 569–574
39 Bailey, C. J., Wilcock, C. and Day, C. (1992) Effect of metformin on glucose metabolism in the splanchnic bed. Br. J. Pharmacol. **105**, 1009–1013
40 Huang, M., Wang, Y., Collins, M., Gu, J. J., Mitchell, B. S. and Graves, L. M. (2002) Inhibition of nucleoside transport by p38 MAPK inhibitors. J. Biol. Chem. **277**, 28364–28367

Received 27 April 2004/23 August 2004; accepted 15 September 2004
Published as BJ Immediate Publication 15 September 2004, DOI 10.1042/BJ20040694